RSC Advances

ROYAL SOCIETY OF CHEMISTRY

www.rsc.org/advances
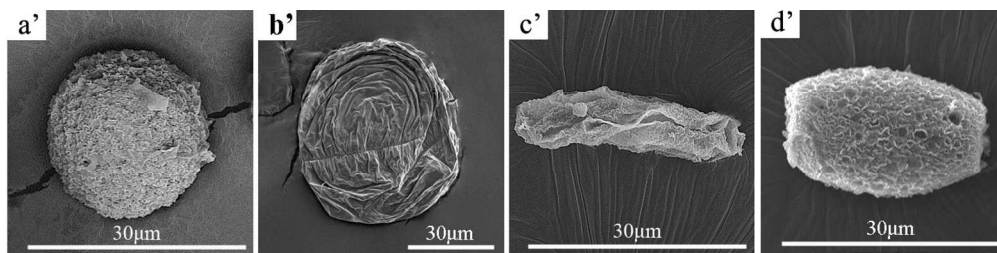
not available yet
122x29mm (300 x 300 DPI)

In-Situ Microfluidic Fabrication of Multi-Shape Inorganic/Organic Hybrid Particles with Controllable Surface Texture and Porous Internal Structure

Guannan Tang, Wenxiu Li, Xiaodong Cao, Hua Dong[*]

National Engineering Research Center for Tissue Restoration and Reconstruction, Department of Biomedical Engineering, School of Materials Science and Engineering, South China University of Technology, Guangzhou, 510641, China

*Corresponding author. E-mail: donghua@scut.edu.cn (H. Dong)

ABSTRACT

In this paper, multi-shape like spherical, ellipsoidal, disklike, and rodlike inorganic/organic hybrid particles are fabricated using droplet-based microfluidics. Instead of photo-polymerization commonly used in the literature, the diversity in particle configuration is realized via the fast hydrolysis of organometallic compound. In comparison to inorganic/organic hybrid particles fabricated by directly incorporating inorganic components in the dispersed phase before droplet formation, our hybrid particles are synthesized in situ because the inorganic component is one of the hydrolysis products, which avoids the agglomeration or precipitation of inorganic components and thus ensures the particle homogeneity. In this paper, we demonstrate the new strategy by using hybrid particle containing poly (lactide-*co*-glycolide) (PLGA) and TiO_2 as a model material, among which TiO_2 is originated from hydrolysis of n-butyl titanate (TBT). The convoluted surface texture of PLGA/TiO_2 particle can be attributed to either the interfacial instabilities of droplets induced by n-butanol as the other hydrolysis product, or elastic-driven wrinkling of the solid film generated on PLGA/TBT droplet surface through TBT hydrolysis. Moreover, due to the presence of hyper-dispersed n-butanol caused by localized TBT hydrolysis in PLGA matrix, porous internal structure can be formed in PLGA/TiO_2 particle. We believe this strategy is versatile to fabricate numerous types of inorganic/organic hybrid particles among which partial or all components can be synthesized through quick hydrolysis of organometallic compounds.

INTRODUCTION

Particle fabrication via droplet-based microfluidics has become world-wide research hotspot in recent years [1-14]. As an important subcategory of microfluidics, droplet-based microfluidics can generate and manipulate discrete droplets with precisely controlled volume and composition through shearing between immiscible phases in microchannels[15]. This technology shows several remarkable advantages: producing monodisperse particles with narrow size distribution, controlling the particle shape and structure in a multiple yet accurate manner, and generating droplets/particles of diverse materials including inorganic compounds, gels, polymers or composites, among which fabrication of nonspherical particles maybe the most attractive one. Owing to the anisotropic configuration, nonspherical particles exhibit unique hydrodynamic, electric, optical, catalytic, or magnetic properties and thus have significant applications in many fields[16-19]. However, most of the particles generated via traditional emulsion methods are spherical due to the minimization of interfacial free energy between the particle and the medium[10]. In contrast, multi-shape particles such as spherical, disklike, rodlike etc have been synthesized in droplet-based microfluidics[20-27], which are often achieved via photo-polymerization reaction in microchannels[22-29]. Although tremendous advanced materials with various shape have been successfully prepared, this strategy cannot be applied to all the materials especially those without photocurable components. Therefore, there is still an urgent need to explore new approaches to fabricate nonspherical particles in droplet-based microfluidics.

In addition to particle shape, composition and porosity are also the fundamental properties of particle materials. Compared with monocomponent particle, hybrid particles can combine the merits of individual components so as to meet the complex requirements from practical applications. For hybrid particles containing inorganic and organic parts, their fabrication in droplet-based microfluidics are normally performed by directly incorporating inorganic particles (such as SiO_2, Fe_3O_4, quantum dots, etc) in the dispersed phase before droplet formation[23,30-32], leading to the severe agglomeration or precipitation of inorganic components and thus poor homogeneity of hybrid particles. Besides, porosity control is another vital factor that should be considered in the particle fabrication process. Addition of porogens has been proven as an effective way[27,33]. However, removal of porogen from particles is time-consuming and the pores

are not uniformly distributed from the inside out.

In this paper, we report a facile microfluidic strategy to fabricate spherical, ellipsoidal, disklike, and rodlike inorganic/organic hybrid particles via hydrolysis of organometallic compound. Specifically, herein we demonstrate the synthesis of a model hybrid particle with TiO_2 as the inorganic component and poly (lactide-*co*-glycolide) (PLGA) as the organic component (in the following section, this hybrid material is labeled as PLGA/TiO_2 particle). The diversity in particle configuration is realized due to the fast hydrolysis of n-butyl titanate (TBT) dissolved in the dispersed phase and the as-formed stiff shell on the droplet surface. As a consequence, the PLGA/TiO_2 particles maintain the shape of liquid droplets in microchannel. Moreover, it is worthy to note that the PLGA/TiO_2 particles are synthesized in situ because the inorganic component TiO_2 is one of the TBT hydrolysis products, which avoids the agglomeration or precipitation of inorganic components and ensures the particle homogeneity. Interestingly, the PLGA/TiO_2 particles display convoluted surface texture and porous internal structure, possibly induced by the other hydrolysis product n-butanol or elastic-driven wrinkling. These particles show great potentials in the areas like drug delivery, biosensing, catalysis, coating, tissue engineering and so forth.

EXPERIMENTAL SECTION

Materials and Reagents. PLGA (Mw=30kDa) with a 50: 50 molar ratio of lactic to glycolic acid was bought from Daigang Company (Zhengzhou, China). TBT and n-butanol were purchased from Fuchen Company (Tianjing, China). Glycerol and poly (vinyl alcohol) (PVA, M_w=88kDa) were purchased from Sinopharm and Aladdin Companies (China), respectively. Negative photoresist (NR21-20000P) was obtained from Futurrex (USA) and polydimethylsiloxane (PDMS, Sylgard 184) was bought from Dow Corning (Midland, USA). All materials and reagents were used as received without further purification.

Fabrication and Surface Treatment of Microfluidic Devices. Microfluidic flow-focusing devices were fabricated via standard soft lithography techniques. In brief, clean silicon wafer was first spin-coated with negative photoresist. After baking at 80^oC for 10 min and 150^oC for 5 min,

the resist was exposed to UV light through a photo-mask and developed in RD6 developer solution. Mixture of PDMS base and curing agent (10:1 w/w) was then poured onto the silicon wafer and cured at 60^oC to make a PDMS replica which was subsequently sealed with a glass slide via O_2 plasma. The width of branch channel and collection channel were 100μm and 250μm, and the depth of all channels was 100μm. Surface treatment was conducted to improve the hydrophilicity of microchannels by injecting PVA/glycerol (2/5 wt%) aqueous solution and curing for 1h.

Microfluidic Fabrication of PLGA/TiO₂ Hybrid Particles. In our study, PLGA and TBT dissolved in dichloromethane were used as the dispersed phase whilst aqueous solution containing 90wt% of glycerol and 0.5wt% of PVA was used as the continuous phase. Both the dispersed phase and continuous phase were injected into the microfluidic devices using syringe pumps (Cole-Parmer, USA). Droplets could be produced continuously at the junction of the microchannels by controlling the flow rates of the dispersed phase and continuous phase. The as-prepared droplets were then collected in 2wt% aqueous solution of PVA (if not otherwise specified), settled at room temperature for 24h, centrifuged at a moderate speed, rinsed thoroughly by deionized water and finally dried in a freeze-drier (Lyophilizer, VIRTIS, USA).

Characterization of PLGA/TiO₂ Hybrid Particles. The morphology of PLGA/TiO₂ hybrid particles was observed using a field emission scanning electron microscope (FE-SEM, NOVA 430, Netherlands). The composition on the particle surface was examined with electron probe micro-analyze (EPMA, EPMA-1610, Shimadzu, Japan) and attenuated total reflection Fourier transform infrared spectroscopy (ATR-FTIR, Nexus Por Euro, USA). The valence state of Ti element was detected via X-ray photoelectron spectrometer (XPS, Axis uHru DCD, England). The structure and content of TBT hydrolysis products in PLGA/TiO₂ hybrid particles was characterized by X-ray diffractometer (XRD, Panalytical, Netherlands), energy-dispersive X-ray spectroscopy (EDS, NOVA 430, Netherlands), thermogravimetric and differential scanning calorimeter (TG-DSC, Diamond, Germany).

RESULTS AND DISCUSSION

Microfluidic flow-focusing devices were employed to generate monodisperse PLGA/TBT droplets, and these droplets were then solidified into PLGA/TiO$_2$ particles under the joint action of a chemical reaction (TBT hydrolysis) and a physical process (solvent extraction). Our primary results reveal that both spherical and nonspherical particles can be obtained. To figure out the inherent mechanism, we fabricated pure PLGA particles under the same conditions except for the removal of TBT from the dispersed phase. The as-prepared PLGA particles are all spherical (Figure S1, supporting information, SI), no matter how to adjust the flow rates of the dispersed phase and continuous phase, indicating the important role of TBT in the fabrication of nonspherical PLGA/TiO$_2$ particles. In our case, two kinds of situation may take place after the formation of PLGA/TBT droplets. If TBT hydrolysis is slower than solvent extraction, PLGA/TBT droplets would maintain liquid state at the outlet of the microfluidic device and become spherical in the collection solution, just like PLGA droplets. On the contrary, if TBT hydrolysis is much faster than solvent extraction, i.e., TBT hydrolysis reaction occurs immediately after droplet formation, a solid shell might be produced on the droplet surface. As a result, the PLGA/TBT droplets can keep their shape in the collection channel even after flowing out of the device. It should be pointed out that the remaining TBT on the droplet surface would undergo more violent hydrolysis in the 2wt% aqueous collection solution of PVA due to the higher concentration of water, and the particle configurations could be further enhanced. In order to verify our presumption, four types of PLGA/TBT droplets with spherical, ellipsoidal, disklike and rodlike morphologies were deliberately generated in microchannel by either controlling the flow rates of the dispersed and continuous phases or changing the size of the collection channel. As shown in Figure 1, the resulting PLGA/TiO$_2$ particles show the same structure as the PLGA/TBT droplets, in good agreement with the second situation.

Different from the traditional microfluidic fabrication of inorganic/organic hybrid particle by mixing inorganic components in the organic dispersed phase, PLGA/TiO$_2$ particles are synthesized in situ because TiO$_2$ is a product of TBT hydrolysis [34, 35]. To confirm the success in hybrid particle preparation, the surface and bulk composition of PLGA/TiO$_2$ particles were first analyzed by EPMA, XPS, FTIR and TG-DSC with the results summarized in Figure 2. Figure 2a

compares the EPMA profiles of PLGA, TiO_2 and $PLGA/TiO_2$ particles prepared in the same device. As can be seen, Ti element is absent from PLGA particle surface but present on TiO_2 and $PLGA/TiO_2$ particle surface, suggesting that Ti is originated from TBT hydrolysis. C and O elements observed on the three sample surfaces can be attributed to PLGA, residual PVA surfactant or TBT hydrolysate. The valence state of Ti in hybrid particle was examined by XPS. The binding energy are 458.4eV and 464.3eV, corresponding to Ti $2p_{3/2}$ and Ti $2p_{1/2}$ of TiO_2 (Figure 2b). This proves that TBT hydrolysis reaction is complete and the hydrolysates are TiO_2 and n-butanol[36]. To investigate the composition of solid shell on hybrid particle surface, ATR-FTIR was performed and the data are shown in Figure 2c. The broad and strong absorption peak at ca. 500~1000 cm^{-1} in curve d' can be assigned to Ti-O-Ti moiety of nanostructured TiO_2 [37]. The absorption bands centered at 1394 and 1611 cm^{-1} can be attributed to the bending vibration of O-H [38], implying the presence of Ti-OH on the TiO_2 particle surface. The broad peak at 2600~3600 cm^{-1} is caused by H_2O. Meanwhile, curve e' shows the characteristic peaks of PLGA including 1000~1450 cm^{-1} (C-H bending vibration), 1746 cm^{-1} (C=O stretching vibration) and 2800~3050 cm^{-1} (C-H stretching vibration). Obviously, peaks belonging to PLGA and TiO_2 can be both found in $PLGA/TiO_2$ hybrid particles (curve f'), and this observation proves that the solid film on $PLGA/TiO_2$ particle surface is composed of PLGA and TiO_2. The little shift of peaks in $PLGA/TiO_2$ particles, compared with those of pure PLGA and TiO_2, is possibly due to the interaction of PLGA and TiO_2 in micro-/nano-scale. Figure 2d shows the TG-DSC curves of $PLGA/TiO_2$ particle. The exothermic peaks at $311^{o}C$ and $417^{o}C$ refer to the combustion of PLGA and phase transition from anatase TiO_2 to rutile TiO_2 (See TG-DSC data of pure PLGA and TiO_2 in Figure S2, SI) [36]. Besides, the morphology and size of TiO_2 in $PLGA/TiO_2$ particle were further characterized via SEM after dissolving PLGA by acetone, and spherical TiO_2 with the size in the range of hundreds of nanometer to several micrometer can be observed (Figure S3). EDS analysis on the cross-section of $PLGA/TiO_2$ particle also reveals that TiO_2 is dispersed both on the particle surface and inside the particle (Table S1).

In addition to the four basic particle shapes, another apparent feature of $PLGA/TiO_2$ particles is their convoluted surface texture. Considering the smooth surface of pure PLGA particles, the wrinkles on the hybrid particle surface can only be resulted from TBT hydrolysis. To our knowledge, the convoluted surface texture was once observed on polystyrene particles by Zhu et

al[10] and the reason was identified as the interfacial instabilities of emulsion droplet induced by n-hexadecanol. Since n-butanol can be in-situ generated as a product of TBT hydrolysis, we can assume that interfacial instabilities of PLGA/TBT droplets are of much possibility to happen. According to the theory developed by Zhu and Hayward[39], n-butanol, as a co-surfactant, can interpenetrate into the PVA monolayer at the organic/water interface and induce the rearrangement of PVA molecules. Hence, the interfacial tension can decrease dramatically or even vanish with the accumulation of n-butanol, driving interfacial roughening of the PLGA/TBT droplets. Our primary results of contact angle measurement also prove the increase of n-butanol in the continuous phase can lead to lower contact angle and thus lower interfacial tension on PLGA/TiO$_2$ particle surface (Table S2, SI). As a consequence, the interfacial area will spontaneously increase by folding or deforming of the interface. Another possible reason for surface roughing is elastic-driven wrinkling [40]. The solid film generated on PLGA/TBT droplet surface by fast hydrolysis of TBT may suffer buckling with the decrease in droplet volume, and thus produce wrinkles on the particle surface. Nevertheless, after solvent extraction and TBT hydrolysis, the wrinkles on the droplet surface can be fixed.

The surface texture of PLGA/TiO$_2$ particles is not unchangeable but can be readily tailored by varying the PLGA and TBT concentrations in the dispersed phase. Take the disklike particle for example, the increase in PLGA concentration leads to a less wrinkled particle surface, as presented in Figure 3. The reason behind this can be understood either from the lower mass percentage of TBT and thus n-butanol in the droplet, decreasing the interfacial roughening speed, or from the smaller volume change between liquid PLGA/TBT droplet and solid PLGA/TiO$_2$ particle, restricting the elastic-driven wrinkling effect. On the other hand, we also changed the TBT concentration whilst kept the PLGA concentration constant. It can be seen from Figure 4 that the surface roughness is enhanced when TBT concentration rises, and highly textured particles can be obtained when TBT concentration is 12mg/g. Although the increase of PLGA concentration or decrease of TBT concentration may both benefit the formation of smoother surface, more PLGA in dispersed phase means bigger particles which reflects in our study as the thickening effects, whereas reduction of TBT doesn't change the particle size too much. This implies that altering TBT concentration maybe a more effective way to control the surface texture of hybrid particle.

More interestingly, in comparison to the sliced PLGA particles in which no pores can be

observed (Figure 5a), PLGA/TiO$_2$ particles display uniform porous internal structure without addition of porogens (Figure 5b). The pore size falls in the range of 0.4~1.2μm and appears invariable regardless of the PLGA concentration (Figure S4 and S5, SI). To identify whether TiO$_2$ or n-butanol play the decisive role, another type of PLGA/TiO$_2$ particles were fabricated using the typical method reported in the literature, i.e., mixing the nanosized TiO$_2$ in the dispersed phase. However, these PLGA/TiO$_2$ particles don't show the same porous structure as anticipated (data not shown here), indicative of little effect of TiO$_2$. In contrast, PLGA particles prepared by directly adding n-butanol in the dispersed phase exhibit porous internal structure but the pores are much larger and unevenly distributed (Figure 5c). Nevertheless, this observation confirms the possibility of n-butanol as a porogen. Although more experiments are still required before drawing a final conclusion, the well-distributed pores in PLGA/TiO$_2$ particles can be ascribed to the dense surface film and localized TBT hydrolysis (or namely, localized generation of n-butanol). As stated above, TBT hydrolysis is initially very fast on the droplet/water interface and then generates a solid surface film. Subsequently, the TBT hydrolysis is slowed down due to the compactness and hydrophobicity of surface film which hinders the diffusion of water into the droplets. In such a case, solvent extraction rate might equal to or even exceed TBT hydrolysis rate, resulting in localized micro-phase separation between solid PLGA and liquid TBT. When water diffuses across the PLGA matrix to the tiny TBT droplets, hydrolysis reaction occurs and generates hyper-dispersed n-butanol. Once the PLGA/TiO$_2$ particles are freeze-dried, the hyper-dispersed n-butanol is volatilized, leaving uniform pore structure. Figure 6 gives the schematic illustration of this process. For those PLGA particles produced after addition of n-butanol, solvent extraction accompanies with the fusion of n-butanol into small droplets inside the particle, which could finally develop into big holes after freeze drying.

In our study, a series of PLGA/TiO$_2$ particles were fabricated with the TiO$_2$ content in the range of 0.1~21.2wt%, and highly TiO$_2$ content can be achieved via the reduction of PLGA concentration (See disklike TiO$_2$ particles without PLGA in Figure S6, SI). Furthermore, it should be pointed out that the strategy developed herein is not limited to the fabrication of multi-shape PLGA/TiO$_2$ particles. Actually, we also replaced PLGA with poly (ε-caprolactone) (PCL) and prepared PCL/TiO$_2$ particles (Figure S7, SI). In a broader perspective, this strategy is versatile to fabricate numerous types of particles among which partial or all components can be synthesized

through quick hydrolysis of organometallic compounds.

CONCLUSION

In summary, we describe the in-situ microfluidic synthesis of multi-shape PLGA/TiO$_2$ hybrid particles with controllable surface texture and porous internal structure. Thanks to the quick TBT hydrolysis, spherical, ellipsoidal, disklike and rodlike PLGA/TiO$_2$ particles can be obtained by controlling the shape of PLGA/TBT droplets in microchannel, which is achieved via the adjustment of flow rates of the dispersed and continuous phases as well as the size of the collection channel. The convolution of particle surface is possibly resulted from either the interfacial instabilities of droplets induced by n-butanol as the other hydrolysis product, or elastic-driven wrinkling of the solid film generated on PLGA/TBT droplet surface through TBT hydrolysis. Moreover, the surface roughness of hybrid particle can be tuned readily by manipulating the relative concentration ratio between PLGA and TBT in the dispersed phase. Due to the presence of hyper-dispersed n-butanol caused by localized TBT hydrolysis, porous internal structure can be generated in PLGA/TiO$_2$ particle. We believe this strategy is suitable to fabricate numerous types of inorganic/organic hybrid particles among which partial or all components can be synthesized through quick hydrolysis of organometallic compounds.

ASSOCIATED CONTENT

* Supporting Information

SEM images of pure PLGA particles, pure TiO$_2$ particles and spherical PCL/TiO$_2$ particles, porous internal structure of PLGA/TiO$_2$ particles, TG-DSC data of pure PLGA and TiO$_2$ particles, morphology and size of TiO$_2$ in PLGA/TiO$_2$ particle, EDS analysis on the cross-section of PLGA/TiO$_2$ particle, contact angle measurement as a function of n-butanol concentration in the continuous phase. This material is available free of charge via the Internet at www.

Notes

The authors declare no competing financial interest.

ACKNOWLEDGEMENTS

REFERENCES

1   A. S. Utada, E. Lorenceau, D. R. Link, P. D. Kaplan, H. A. Stone and D. A.Weitz, *Science,* 2005, **308**, 537.

2   C. Liang-Yin, A. S. Utada, R. K.Shah, K. Jin-Woong and D. A Weitz, *Angew. Chem. Int. Edit*, 2007, **46**,8970.

3   K. Shin-Hyun and D. A. Weitz, *Angew. Chem. Int. Edit*, 2011, **50**, 8731.

4   T. Nisisako, S. Okushima and T. Torii, *Soft Matter*, 2005, **1**, 23.

5   M. Seo, C. Paquet, Z. H. Nie, S. Q. Xu and E. Kumacheva *Soft Matter*, 2007, **3**, 986.

6   J. Y. Wang, Y. D. Hu, R. H. Deng, W. J. Xu, S. Q. Liu, R. J. Liang, Z. H.Nie and J. T. Zhu, *Lab Chip,* 2012, **12**, 2795.

7   Y. H. Chen, G. Nurumbetov, R. Chen, N. Ballard and S. A. F. Bon, *Langmuir,* 2013, **29**, 12657.

8   Y. H. Wang, E. Tumarkin, D. Velasco, M. Abolhasani, W. Lau and E. Kumacheva, *Lab Chip,* 2013, **13**, 2547.

9   Y. Liu, M. H.Ju, C. Q. Wang, L. X. Zhang and X. Q. Liu, *J. Mater. Chem,* 2011, **21**, 15049.

10   S. Q. Liu, R. H. Deng, W. K. Li and J. T. Zhu, *Adv. Funct.Mater,* 2012, **22**, 1692.

11   S. Y. Teh, R. Khnouf, H.Fan and A. P. Lee, *Biomicrofluidics,* 2011, **5**, 44113.

12   Y. C. Pan, M. H. Ju, C. Q. Wang, L. X. Zhang and N. P. Xu, *Chem.Commun,* 2010, **46**, 3732.

13   S. Ota, S. Yoshizawa and S.Takeuchi, *Angew. Chem. Int. Edit,* 2009, **48**, 6533.

14   N. Prasad, J. Perumal, C. H. Choi, C. S. Lee and D. P. Kim, *Adv. Funct. Mater,* 2009, **19**, 1656.

15   J. T. Wang, J. Wang and J. J. Han, *Small,* 2011, **7**, 1728.

16   C. Burda, X. B. Chen, R.Narayanan and M.A. El-Sayed, *Chem. Rev,* 2005, **105**, 1025.

17   G. Hodes, *Adv. Mater,* 2007, **19**, 639.

18   G. M. Whitesides, *Small,* 2005, **1**, 172.

19   Y. Xia, P. Yang, Y. Sun, Y. Wu, B. Mayers, B. Gates, Y. Yin, F. Kim and H. Yan, *Adv. Mater,* 2003, **15**, 353.

20   S. Sugiura, T. Oda, Y. Izumida, Y. Aoyagi, M. Satake, A. Ochiai, N. Ohkohchi and M. Nakajima, *Biomaterials,* 2005, **26**, 3327.

21   W. H. Tan, S. Takeuchi, *Adv. Mater,* 2007, **19**, 2696.

22   D. Dendukuri, K. Tsoi, T. A. Hatton and P. S. Doyle, *Langmuir,* 2005, **21**, 2113.

23   S. Q. Xu, Z. H. Nie, M. Seo, P. Lewis, E. Kumacheva, H. A. Stone, P. Garstecki, D. B. Weibel, I. Gitlin, and
        G. M. Whitesides, *Angew. Chem. Int. Edit,* 2005, **44**, 724.

24   Z. H. Nie, W. Li, M. Seo, S. Q. Xu and E. Kumacheva, *J. Am. Chem. Soc,* 2006, **128**, 9408.

25   D. K. Hwang, D. Dendukuri and P. S. Doyle, *Lab Chip,* 2008, **8**, 1640.

26   R. F. Shepherd, J. C. Conrad, S. K. Rhodes, D. R. Link, M. Marquez, D. A. Weitz and J. A. Lewis,
        Langmuir, 2006, **22**, 8618.

27   A. Abbaspourrad, N. J. Carroll, S. H. Kim and D. A. Weitz, *Adv. Mater,* 2013, **25**, 3215.

28   S. N. Yin, C. F. Wang, Z. Y. Yu, J. Wang, S. S. Liu and S. Chen, *Adv. Mater,* 2011, **23**, 2915.

29   S. Seiffert, M. B. Romanowsky and D. A. Weitz, *Langmuir,* 2010, **26**, 14842.

30   Y. J. Jiang, J. H. Jiang, Q. M. Gao, M. L. Ruan, H. M. Yu and L. J. Qi, *Nanotechnology,* 2008, **19**, 075714.

31   S. I. Stoeva, F. W. Huo, J. S. Lee and C. A. Mirkin, *J. Am. Chem.l Soc,* 2005, **127**, 15362.

32   D. L. Shi, H. S. Cho, Y. Chen, H. Xu, H. C. Gu, J. Lian, W. Wang, G. K. Liu, C. Huth, L. M.Wang, R. C.
        Ewing, S. Budko, G. M. Pauletti and Z. Y. Dong, *Adv. Mater,* 2009, **21**, 2170.

33   S. Dubinsky, H. Zhang, Z. H. Nie, I. Gourevich, D. Voicu, M. Deetz and E. Kumacheva,
        *Macromolecules ,*2008, **41**, 3555.

34   S. A. Khan and K. F. Jensen, *Adv. Mater*. 2007, **19**, 2556.

35   M. Takagi, T. Maki, M. Miyahara and K. Mae, *Chem. Eng. J.* 2004, **101**, 269.

36   J. H. Tian, P. F. Gao, Z. Y. Zhang, W. H. Luo and Z. Q. Shan, *Int. J. Hydrogen Energ,* 2008, **33**, 5686.

37   J. F. Ye, W. Liu, J.G. Cai, S. Chen, X.W. Zhao, H.H. Zhou and L.M. Qi, *J. Am. Chem. Soc,* 2011, **133**, 933.

38   J. Das, F. S. Freitas, I. R. Evans, A. F. Nogueirab and D. Khushalani, *J. Mater. Chem.* 2010, **20**, 4425.

39   J.T. Zhu and R.C. Hayward, *Angew. Chem. Int. Ed,* 2008, **130**, 7496.

40   Y. Sugiyama, R. J. Larsen, J.W. Kim, and D. A. Weitz, *Langmuir,* 2006, **22**, 6024.
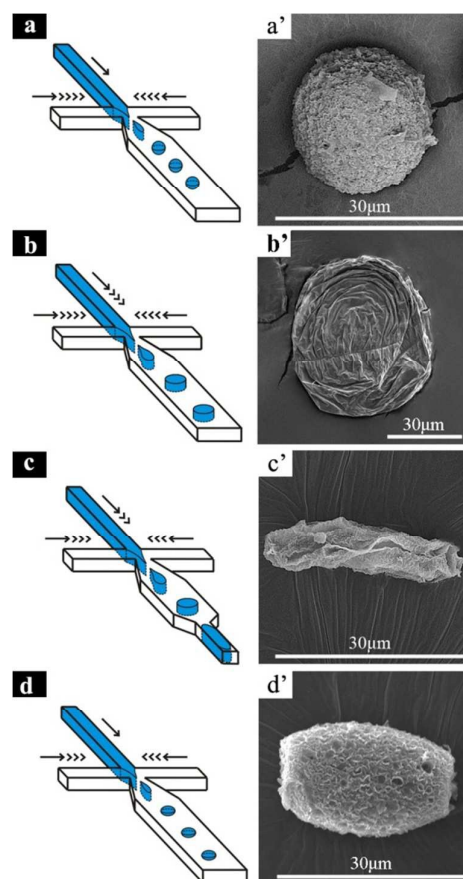
Figures

Figure 1

Figure 1. Schematic (a–d) and SEM images (a'- d') of PLGA/TiO$_2$ particles with multiple shapes: (a, a') spherical; (b, b') disklike; (c, c') rodlike and (d, d') ellipsoidal. Particle shape was determined by the relative ratio of the diameter d of the PLGA/TBT droplets to each dimension (w: width; h: height; w > h) of the collection channel: when $w > d$ and $h > d$ (Fig.1a, a'), spherical particles were generated; when $w > d$ and $h < d$, disklike particles were produced (Fig.1b, b'); and when $w < d$ and $h < d$, rodlike particles were made (Fig.1c, c'). Ellipsoidal particles were obtained under a large flow rate of the continuous phase. The diameter d of PLGA/TBT droplets was adjusted by controlling the flow rates of the dispersed and continuous phases with the ratio indicated using arrows in the figure. Meanwhile, the width and height of the collection channel were changed by the mask of photolithography. Please note that the microfluidic devices used in a-c were the same, i.e., the width of branch channel and collection channel were 100μm and 250μm, and the depth of all channels was 100μm. The microchannel in d was similar to those of a-c except that the collection channel was narrowed near the outlet (the width was reduced from 250μm to 100μm).
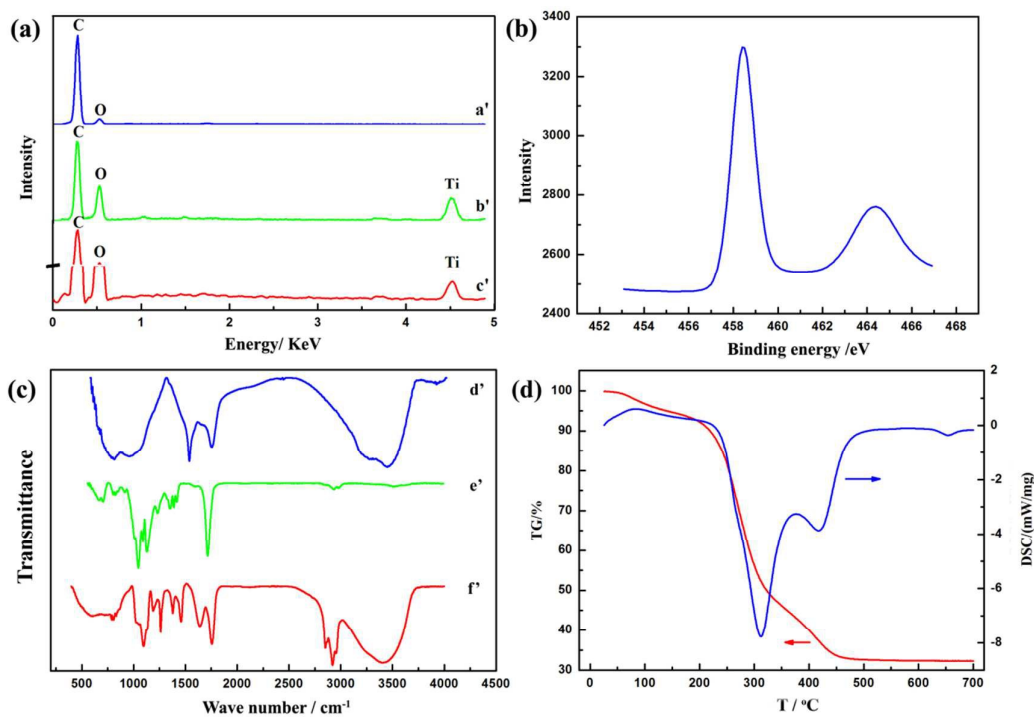
Figure 2

Figure 2. Surface and bulk composition analysis and characterization of PLGA/TiO$_2$ particles: (a) EPMA profiles of (a') PLGA, (b') TiO$_2$, (c') PLGA/TiO$_2$; (b) XPS data of PLGA/TiO$_2$ particles; (c) ATR-FTIR spectra of (d') TiO$_2$, (e') PLGA, (f') PLGA/TiO$_2$; (d) TG-DSC curves for PLGA/TiO$_2$. All the samples were collected using the same microfluidic devices, except that the dispersed phases were pure PLGA, pure TBT and PLGA/TBT dissolved in dichloromethane. Note that the PLGA/TiO$_2$ particles used in a and b were prepared using a dispersed phase containing 8mg/g TBT and 30mg/g PLGA, whilst the PLGA/TiO$_2$ particles used in c and d were prepared using a dispersed phase containing 8mg/g TBT and 7mg/g PLGA.
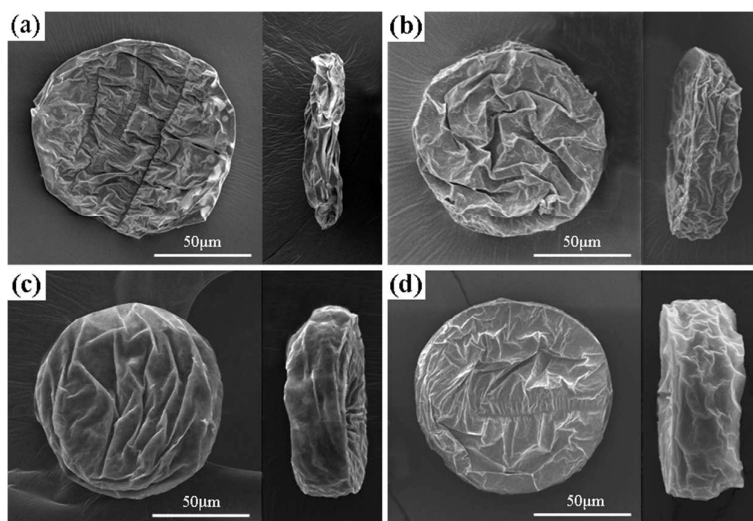
Figure 3

Figure 3. SEM images of PLGA/TiO$_2$ particles fabricated with the dispersed phase containing constant TBT concentration (8mg/g) and various PLGA concentrations: (a) 10 mg/g; (b) 30 mg/g; (c) 50 mg/g; (d) 70 mg/g. The continuous phase was aqueous solution containing 90wt% of glycerol and 0.5wt% of PVA, and the collection solution was 2wt% aqueous solution of PVA. The thickness of PLGA/TiO$_2$ particles in a-d is 14.7, 23.5, 29.4 and 38.2μm, respectively.
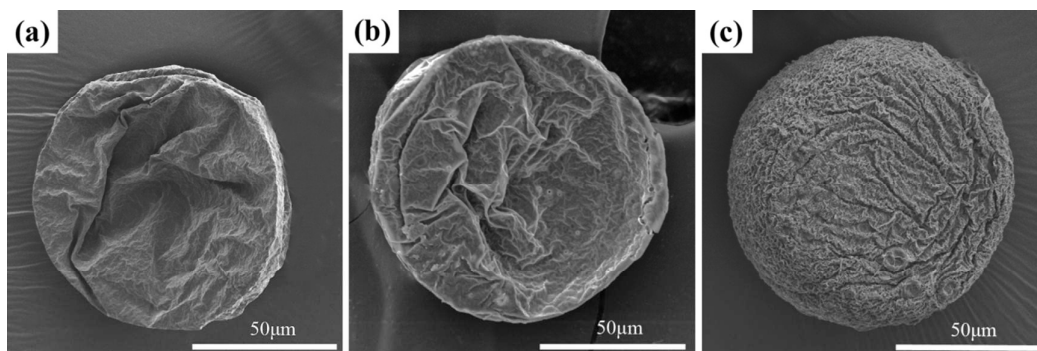
Figure 4

Figure 4. SEM images of PLGA/TiO$_2$ particles fabricated with the dispersed phase containing constant PLGA concentration (30mg/g) and various TBT concentrations: (a) 4 mg/g; (b) 8 mg/g; (c) 12 mg/g. The continuous phase was aqueous solution containing 90wt% of glycerol and 0.5wt% of PVA, and the collection solution was 2wt% aqueous solution of PVA. The particle thickness in a-c is similar (~22-25μm).
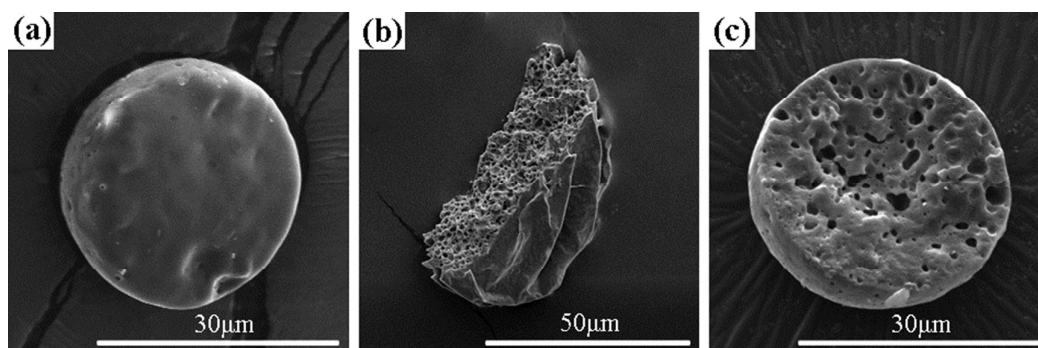
Figure 5

Figure 5. Cross-section SEM images of sliced particles. These particles were fabricated using the dispersed phases containing (a) PLGA, (b) PLGA and TBT, (c) PLGA and n-butanol. The concentrations of PLGA, TBT and n-butanol were 70 mg/g, 8mg/g and 7mg/g, respectively. The concentration of n-butanol was calculated from that of TBT based on hydrolysis reaction equation.
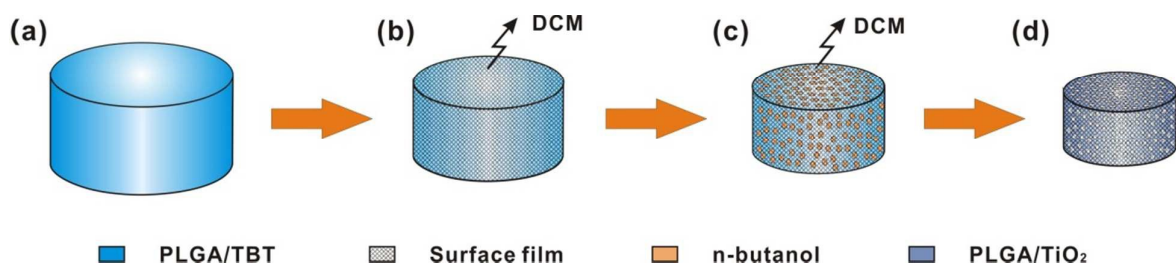
Figure 6

Figure 6. Schematic illustration on the formation mechanism of porous internal structure inside disklike PLGA/TiO$_2$ particles. (a) PLGA/TBT droplets are first produced at the junction of microchannels; (b) TBT hydrolysis occurs on the droplet/water interface and a solid film is generated; (c) hyper-dispersed n-butanol is resulted from the localized TBT hydrolysis in PLGA matrix; (d) porous internal structure is formed via freeze-drying process in which n-butanol is volatilized.
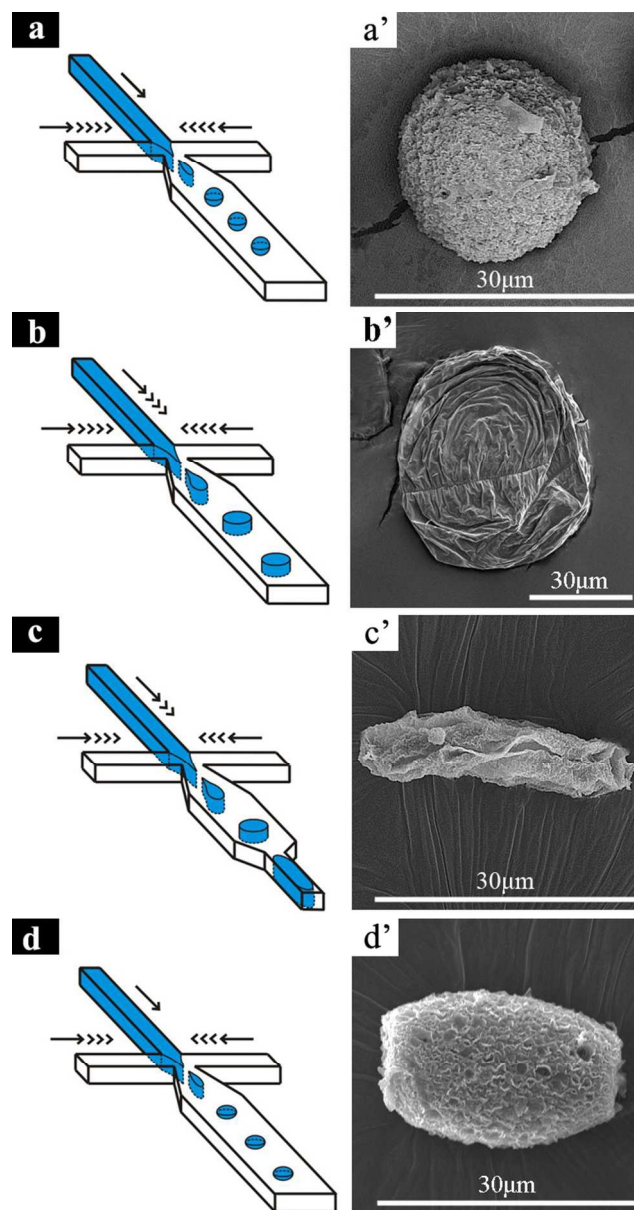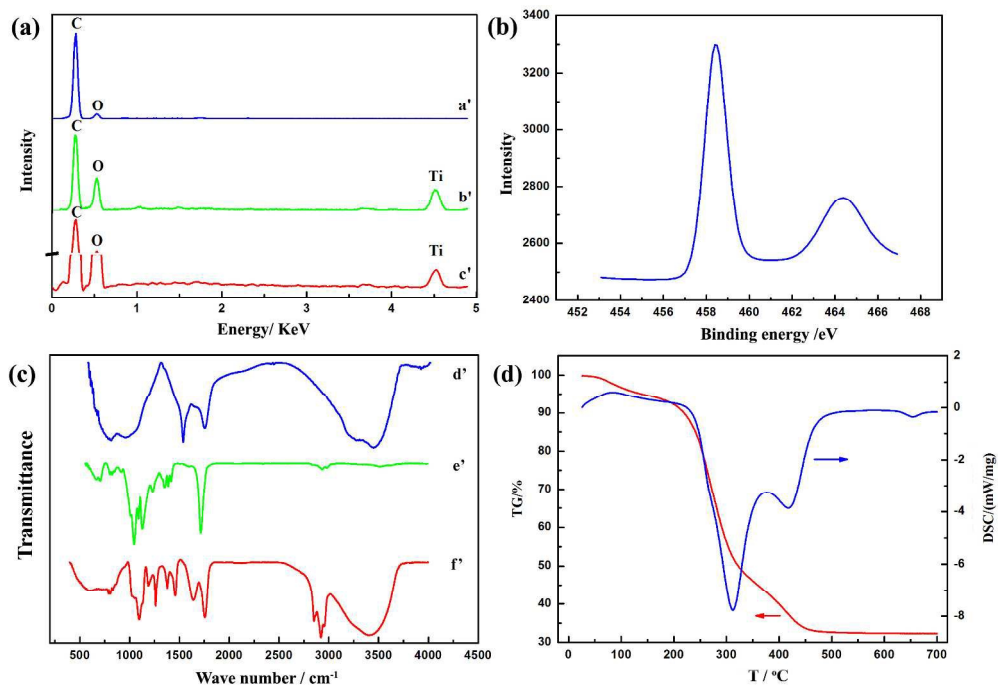
Figure 1. Schematic (a–d) and SEM images (a'- d') of PLGA/TiO2 particles with multiple shapes: (a, a') spherical; (b, b') disklike; (c, c') rodlike and (d, d') ellipsoidal. Particle shape was determined by the relative ratio of the diameter d of the PLGA/TBT droplets to each dimension (w: width; h: height; w > h) of the collection channel: when w > d and h > d (Fig.1a, a'), spherical particles were generated; when w > d and h < d, disklike particles were produced (Fig.1b, b'); and when w < d and h < d, rodlike particles were made (Fig.1c, c'). Ellipsoidal particles were obtained under a large flow rate of the continuous phase. The diameter d of PLGA/TBT droplets was adjusted by controlling the flow rates of the dispersed and continuous phases with the ratio indicated using arrows in the figure. Meanwhile, the width and height of the collection channel were changed by the mask of photolithography. Please note that the microfluidic devices used in a-c were the same, i.e., the width of branch channel and collection channel were 100µm and 250µm, and the depth of all channels was 100µm. The microchannel in d was similar to those of a-c except that the collection channel was narrowed near the outlet (the width was reduced from 250µm to 100µm).
64x122mm (300 x 300 DPI)

508x347mm (150 x 150 DPI)

Figure 3. SEM images of PLGA/TiO2 particles fabricated with the dispersed phase containing constant TBT concentration (8mg/g) and various PLGA concentrations: (a) 10 mg/g; (b) 30 mg/g; (c) 50 mg/g; (d) 70 mg/g. The continuous phase was aqueous solution containing 90wt% of glycerol and 0.5wt% of PVA, and the collection solution was 2wt% aqueous solution of PVA. The thickness of PLGA/TiO2 particles in a-d is 14.7, 23.5, 29.4 and 38.2µm, respectively.µµµµµµµµµµµvµµµµµµ
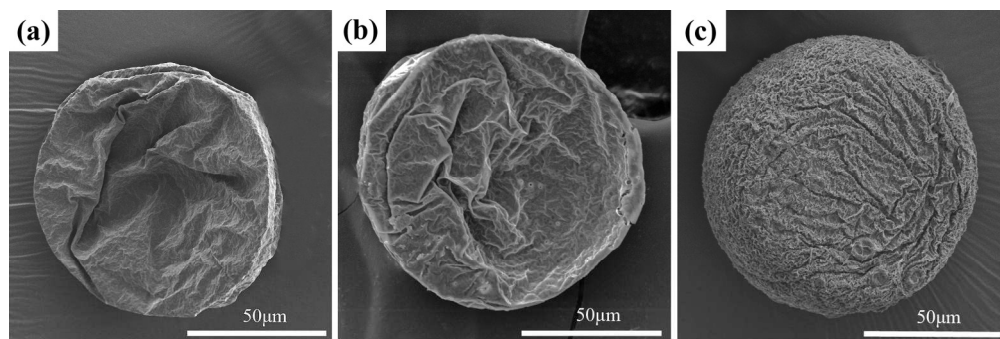296x201mm (72 x 72 DPI)

Figure 4. SEM images of PLGA/TiO2 particles fabricated with the dispersed phase containing constant PLGA concentration (30mg/g) and various TBT concentrations: (a) 4 mg/g; (b) 8 mg/g; (c) 12 mg/g. The continuous phase was aqueous solution containing 90wt% of glycerol and 0.5wt% of PVA, and the collection solution was 2wt% aqueous solution of PVA. The particle thickness in a-c is similar (~22-25μm).
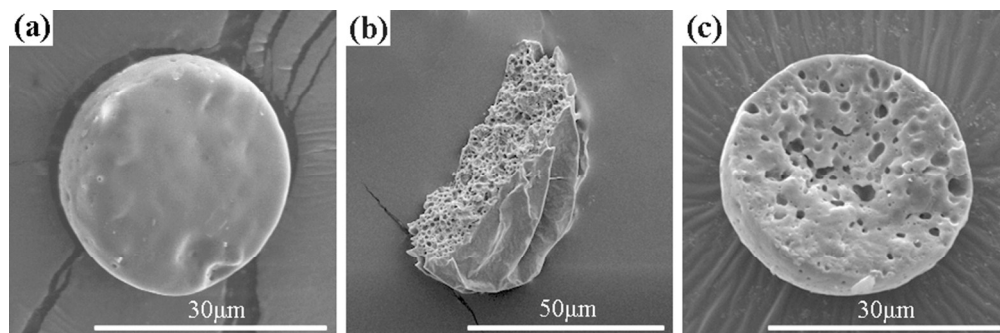
660x220mm (72 x 72 DPI)

Figure 5. Cross-section SEM images of sliced particles. These particles were fabricated using the dispersed phases containing (a) PLGA, (b) PLGA and TBT, (c) PLGA and n-butanol. The concentrations of PLGA, TBT and n-butanol were 70 mg/g, 8mg/g and 7mg/g, respectively. The concentration of n-butanol was calculated from that of TBT based on hydrolysis reaction equation.
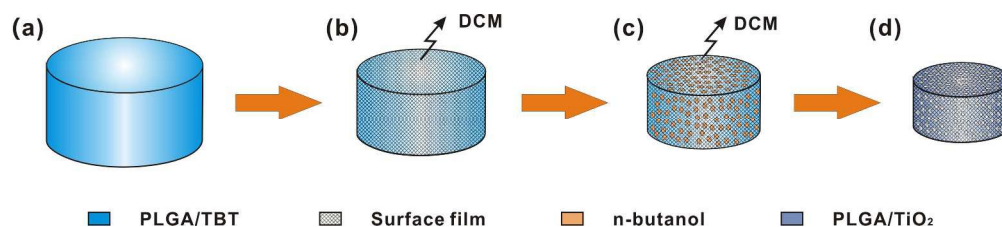335x110mm (72 x 72 DPI)

Figure 6. Schematic illustration on the formation mechanism of porous internal structure inside disklike PLGA/TiO2 particles. (a) PLGA/TBT droplets are first produced at the junction of microchannels; (b) TBT hydrolysis occurs on the droplet/water interface and a solid film is generated; (c) hyper-dispersed n-butanol is resulted from the localized TBT hydrolysis in PLGA matrix; (d) porous internal structure is formed via freeze-drying process in which n-butanol is volatilized.

267x56mm (300 x 300 DPI)